tvst

Cornea & External Disease

How Modifications of Corneal Cross-Linking Protocols Influence Corneal Resistance to Enzymatic Digestion and Treatment Depth

Malwina Kowalska[1–3,*], Elisa Mischi[2,3,*], Szymon Stoma[4], Simon F. Nørrelykke[4,5], Sonja Hartnack[1], and Simon A. Pot[2]

[1] Section of Epidemiology, Vetsuisse Faculty, University of Zurich, Switzerland
[2] Ophthalmology Section, Equine Department, Vetsuisse Faculty, University of Zurich, Switzerland
[3] Center for Clinical Studies, Vetsuisse Faculty, University of Zurich, Switzerland
[4] Image and Data Analysis Group (IDA), Scientific Center for Optical Electron Microscopy (ScopeM), Swiss Federal Institute of Technology (ETH), Zurich, Switzerland
[5] Department of Systems Biology, Harvard Medical School, Boston, MA, USA

Correspondence: Simon A. Pot, Ophthalmology Section, Vetsuisse Faculty, University of Zurich, Winterthurerstrasse 260, 8057 Zurich, Switzerland.
e-mail: spot@vetclinics.uzh.ch

Received: October 7, 2022
Accepted: April 3, 2023
Published: May 16, 2023

Keywords: photoactivated chromophore for keratitis corneal cross-linking (PACK-CXL); infectious keratitis; ex vivo; acceleration; fluence

Citation: Kowalska M, Mischi E, Stoma S, Nørrelykke SF, Hartnack S, Pot SA. How modifications of corneal cross-linking protocols influence corneal resistance to enzymatic digestion and treatment depth. Transl Vis Sci Technol. 2023;12(5):18, https://doi.org/10.1167/tvst.12.5.18

Purpose: The purpose of this study was to determine the effects of the Photoactivated Chromophore for Keratitis Corneal Cross-Linking (PACK-CXL) protocol modifications on corneal resistance to enzymatic digestion and treatment depth.

Methods: Eight hundred one ex vivo porcine eyes were randomly divided into groups of 12 to 86 corneas, treated with various epi-off PACK-CXL modifications, including acceleration (30 > 2 minutes, 5.4 J/cm^2), increased fluence (5.4 > 32.4 J/cm^2), deuterium oxide (D_2O) supplementation, different carrier types (dextran versus hydroxypropyl methylcellulose [HPMC]), increased riboflavin concentration (0.1 > 0.4%), and riboflavin replenishment during irradiation (yes/no). Control group eyes did not receive PACK-CXL. A pepsin digestion assay was used to determine corneal resistance to enzymatic digestion. A phalloidin fluorescent imaging assay was used to determine the PACK-CXL treatment effect depth. Differences between groups were evaluated using a linear model and a derivative method, respectively.

Results: PACK-CXL significantly increased corneal resistance to enzymatic digestion compared to no treatment ($P < 0.03$). When compared to a 10 minute, 5.4 J/cm^2 PACK-CXL protocol, fluences of 16.2 J/cm^2 and higher increased corneal resistance to enzymatic digestion by 1.5- to 2-fold ($P < 0.001$). Other protocol modifications did not significantly change corneal resistance. A 16.2 J/cm^2 fluence also increased collagen compaction in the anterior stroma, whereas omitting riboflavin replenishment during irradiation increased PACK-CXL treatment depth.

Conclusions: Increasing fluence will likely optimize PACK-CXL treatment effectiveness. Treatment acceleration reduces treatment duration without compromising effectiveness.

Translational Relevance: The generated data help to optimize clinical PACK-CXL settings and direct future research efforts.

Introduction

The two main current indications for corneal cross-linking (CXL) are the treatment of keratoconus in human patients and the treatment of infectious keratitis in both human and veterinary patients.[1–5]

An imbalance in matrix metalloproteinase (MMP) and tissue inhibitor of metalloproteinase (TIMP) activity in the corneal stroma is an important factor in the disease pathology and progression of both keratoconus[6–8] and infectious keratitis,[9–15] albeit on a vastly different timescale. Keratoconus typically demonstrates a disease progression over decades.[16,17]

Whereas infectious keratitis is a much more aggressive disease, where the process of corneal tissue destruction can rapidly progress within several hours to days,[11,18,19] typically with a bacterial or fungal component present.[20–23]

Due to the clear difference in disease progression between keratoconus and infectious keratitis, the use of routine keratoconus-tailored CXL protocols may be insufficient for the treatment of infectious keratitis.[24] A 30 minute, 3 mW, 5.4 J/cm^2 single fluence (energy dose) CXL protocol, using 0.1% riboflavin in 20% dextran as chromophore solution, and 365 nm UV-A light as energy source, named the "Dresden protocol," was originally designed for the treatment of keratoconus in human patients.[25–28] Changes, including collagen compaction, keratocyte apoptosis, and the appearance of a demarcation line, have been observed in the anterior half to two-thirds of the corneal stroma after CXL treatment.[28–33]

CXL stiffens the corneal stroma and improves corneal stromal resistance to enzymatic digestion by creating cross-links within collagen fibrils, and between collagen fibrils and other corneal stromal matrix components.[34–39] As such, CXL is used to stabilize the corneal stroma and prevent disease progression in corneas affected by keratoconus and infectious keratitis. Another goal for CXL treatment of infectious keratitis, is the antimicrobial effect,[40–42] which can be increased by adapting the CXL protocol, especially by increasing fluence.[43]

The clinical use of CXL for infectious keratitis was renamed "Photoactivated Chromophore for Keratitis – Corneal Cross-Linking" (PACK-CXL), to indicate this specific indication for use, but also to create room for protocol adaptations by the use of other, potentially more efficient, chromophores and energy sources.[24] Recently, a randomized controlled clinical trial demonstrated that standalone PACK-CXL may be an alternative to antimicrobial drug therapy as first-line treatment for infectious keratitis.[44] However, PACK-CXL is currently not recommended as solo treatment for infectious keratitis.

Various PACK-CXL protocol modifications are easy to implement in a clinical setting, and accelerated, high fluence protocols, intended to increase clinical effectiveness, are especially popular, as demonstrated in a number of clinical studies.[45–50]

However, a clear knowledge gap exists regarding the effects of PACK-CXL protocol modifications on the induced level of resistance to enzymatic digestion, and the depth of this effect within the corneal stroma. Because these end points may dictate treatment results, PACK-CXL protocol modifications have the potential to affect treatment success.

We hypothesize that the PACK-CXL protocol modifications illustrated in Figure 1 will either increase or decrease crosslink density, and/or treatment depth, ex vivo. See Supplement A, and Figure 1 and legend, for a comprehensive explanation.

Repeated testing is needed to prove theoretical principles and gain confidence in existing evidence regarding proposed PACK-CXL protocol modifications, especially prior to routine clinical use. We therefore aimed to evaluate the impact of various new and previously tested PACK-CXL protocols on corneal stromal resistance to enzymatic digestion and treatment effect depth (see Fig. 1). To determine whether our postulates detailed in Figure 1 are correct, we used previously described ex vivo porcine cornea pepsin digestion and phalloidin fluorescent imaging assays.[31,38,51,52]

Materials and Methods

Detailed experimental protocols are available as Supplement B.

PACK-CXL Procedure

Porcine eyes were obtained from the local abattoir and processed within 10 hours of slaughter. Only eyes with normal anterior segment, based upon focal light source examination, were included. Similar to previously reported methods,[53–55] corneas were first de-epithelialized, then saturated with a riboflavin solution (see Tables 1a, 1b for details of the chromophore solutions used in the various experiments), and irradiated with an 11 mm (pepsin digestion assay) or 8 mm (fluorescent imaging assay) diameter beam of 365-nm UVA light (PXL Velvet 345; Peschke Trade GmbH, Switzerland). Excess riboflavin was removed prior to irradiation and replenished during and between irradiation cycles, except for the no riboflavin replenishment group. Eyes in the control group were de-epithelialized but did not receive riboflavin or UVA irradiation. The PACK-CXL protocol details are presented in Tables 1a and 1b, and Figure 2 illustrates the experimental protocols. Central corneal thickness (CCT) was measured by ultrasound pachymeter (PachPen; Accutome) at two time points: after de-epithelialization and after saturation with riboflavin. In accordance with previously published protocols,[53–55] and to reduce the variance in corneal hydration prior to UVA irradiation, the duration of riboflavin saturation was adjusted to the CCT measurements after de-epithelialization. Corneas with a CCT under 750 µm, between 751 and 800 µm, and exceeding 800 µm, were saturated with riboflavin in

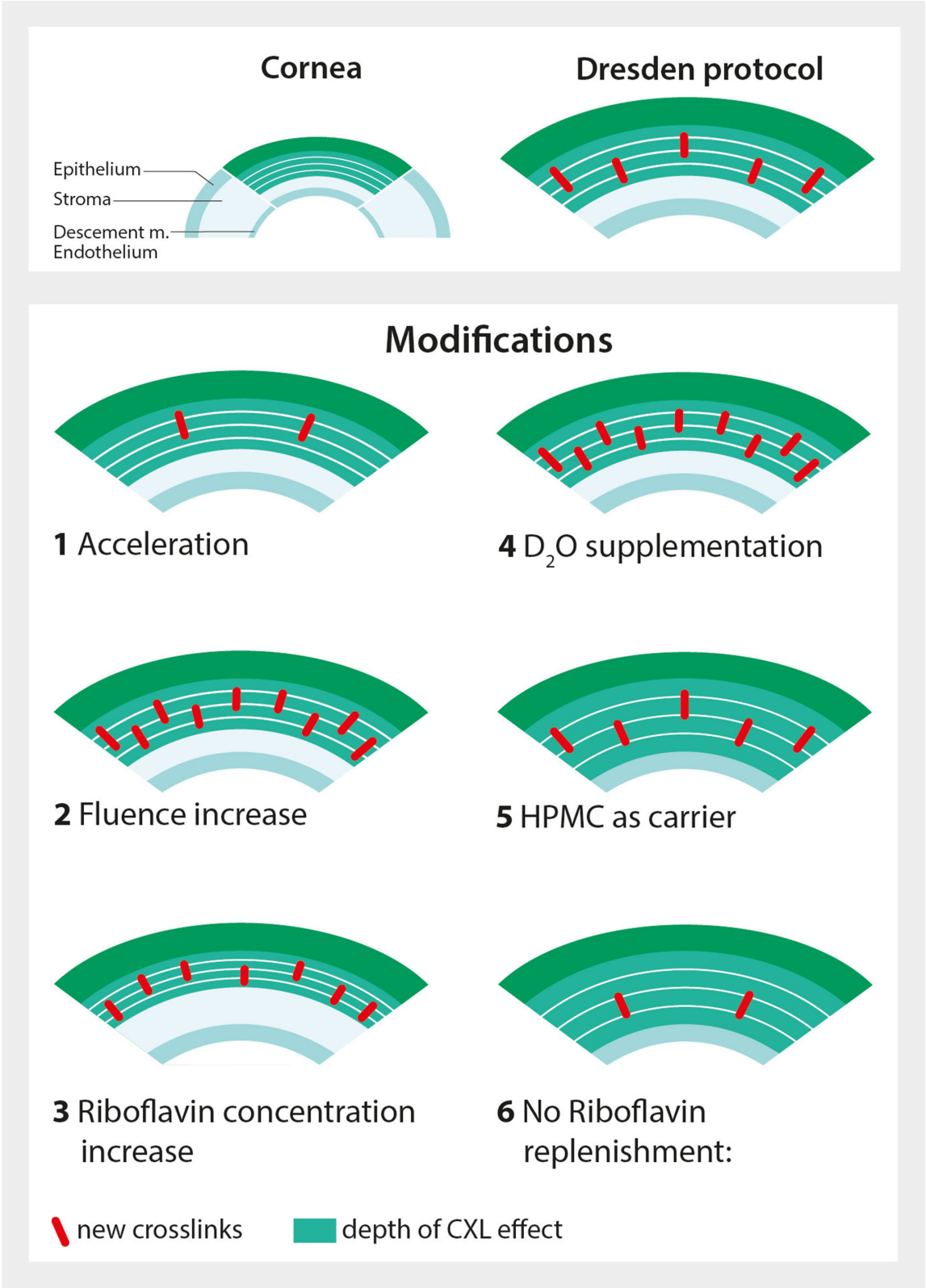

Figure 1. Hypothetical effects of PACK-CXL protocol modifications on the induced corneal stromal crosslink density and treatment effect depth. The Dresden CXL protocol induces crosslinks in the corneal stroma with an observed treatment effect in the anterior half to two-thirds of the cornea. Various PACK-CXL protocol modifications are easy to implement in a clinical setting, and have the following reported and hypothetical effects: (1) Acceleration decreases treatment time and facilitates the delivery of higher fluences: we hypothesize a reduced crosslink density, and unchanged treatment depth. (2) Higher fluences increase antibacterial efficacy[40,41,43,76] and stromal stability[52]: we hypothesize an increased crosslink density, and unchanged treatment depth. (3) Higher riboflavin concentrations theoretically →

←

focus the PACK-CXL effect in the superficial stroma,[86] and increase stromal stability[56,82,86–88]: we hypothesize an increased crosslink density, and reduced treatment depth. (4) D_2O supplementation enhances the half-life of singlet oxygen[89]: we hypothesize an increased crosslink density, and unchanged treatment depth. (5) HPMC as carrier can help to drive riboflavin deep into the corneal tissue[90]: we hypothesize an unchanged crosslink density, and increased treatment depth. (6) Avoiding riboflavin replenishment during irradiation may allow riboflavin concentrations in the superficial stroma to decrease, and UVA to reach deeper layers with high riboflavin concentrations[82]: we hypothesize a reduced crosslink density, and increased treatment depth. Note that these graphs are simplified visual representations, and that the illustrated corneal stromal crosslink densities do not represent real crosslink densities. All hypothesized protocol modification effects are comparisons to the Dresden protocol.

Table 1a. PACK-CXL Protocol Details: Pepsin Digestion Assay

Experiments	Fluence [J/cm^2]	Intensity [mW/cm^2]	Total Irradiation Time [min]	Chromophore				Sample Size
				Type	Concentration	Carrier	Replenishment	
1: Acceleration								
Control	0	0	0	–	–	–	–	28
30 min	5.4	3	30	Riboflavin	0.1%	Dextran	yes	36
10 min	5.4	9	10	Riboflavin	0.1%	Dextran	yes	36
2 min	5.4	45	2	Riboflavin	0.1%	Dextran	yes	35
2: Fluence								
Control	0	0	0	–	–	–	–	59
5.4 J/cm^2	5.4	9	10	Riboflavin	0.1%	Dextran	yes	30
10.8 J/cm^2	10.8	$9 + 45$	12	Riboflavin	0.1%	Dextran	yes	30
16.2 J/cm^2	16.2	$9 + 2 \times 45$	14	Riboflavin	0.1%	Dextran	yes	30
21.6 J/cm^2	21.6	$9 + 3 \times 45$	16	Riboflavin	0.1%	Dextran	yes	56
27 J/cm^2	27	$9 + 4 \times 45$	18	Riboflavin	0.1%	Dextran	yes	29
32.4 J/cm^2	32.4	$9 + 5 \times 45$	20	Riboflavin	0.1%	Dextran	yes	29
3: Riboflavin concentration and D_2O supplementation								
Control	0	0	0	–	–	–	–	25
0.1 Riboflavin	5.4	9	10	Riboflavin*	0.1%	Dextran	yes	25
0.1 Riboflavin + D_2O	5.4	9	10	Riboflavin*	0.1%	Dextran + 30% D_2O	yes	25
0.4 Riboflavin	5.4	9	10	Riboflavin*	0.4%	Dextran	yes	25
0.4 Riboflavin + D_2O	5.4	9	10	Riboflavin*	0.4%	Dextran + 30%D_2O	yes	25
4: Riboflavin carrier								
Control	0	0	0	–	–	–	–	38
HPMC	5.4	9	10	Riboflavin	0.1%	HMPC	yes	42
Dextran	5.4	9	10	Riboflavin	0.1%	Dextran	yes	42
5: Riboflavin replenishment								
Control	0	0	0	–	–	–	–	13
Yes	16.2	$9 + 2 \times 45$	14	Riboflavin	0.1%	Dextran	yes	14
No	16.2	$9 + 2 \times 45$	14	Riboflavin	0.1%	Dextran	no	14

*Commercial product not available, prepared by pharmacist. Two commercial products used: Riboflavin solution for Corneal Cross-Linking (CXL), Peschke D, PESCHKE Trade GmbH, Huenenberg, Switzerland; and Riboflavin solution for Corneal Cross-Linking (CXL), Peschke M, PESCHKE Trade GmbH, Huenenberg, Switzerland.

20% dextran for 20 minutes, 25 minutes, or 30 minutes, respectively.

Pepsin Digestion Assay

After PACK-CXL treatment, full-thickness corneal buttons with an 8 mm diameter were removed with a skin biopsy punch from the center of the irradiated area and placed in 5 mL tubes containing 4 mL of a 5% pepsin solution (Pepsin from porcine gastric mucosa, powder, ≥500 U/mg; SIGMA, catalog no. 77160) at a pH of 1.1.

Samples were incubated in the oven (Hybridization Oven/Shaker; Amersham Life Science) at 25°C, shaken every other day and monitored for signs of digestion until measurement of the dry weight at day 8 (DW8) or 16 (DW16) after incubation. Dry weight measure-

Table 1b. PACK-CXL Protocol Details: Fluorescent Imaging Assay

Treatment Group	Fluence [J/cm^2]	Intensity [mW/cm^2]	Total Irradiation Time [min]	Chromophore				Sample Size
				Type	Concentration	Carrier	Replenishment	
Control epi-on	–	–	–	–	–	–	–	25
Control epi-off	–	–	–	–	–	–	–	86
Fluence 5.4 J/cm^2	5.4	9	10	Riboflavin	0.1%	Dextran	yes	33
Fluence 5.4 J/cm^2; 0.4.% riboflavin	5.4	9	10	Riboflavin*	0.4%	Dextran	yes	14
Fluence 5.4 J/cm^2; HPMC	5.4	9	10	Riboflavin	0.1%	HPMC	yes	12
Fluence 16.2 J/cm^2	16.2	$9 + 2 \times 45$	14	Riboflavin	0.1%	Dextran	yes	14
Fluence 16.2 J/cm^2; no riboflavin replenishment	16.2	$9 + 2 \times 45$	14	Riboflavin	0.1%	Dextran	no	12

Epi-on: corneal epithelium intact; Epi-off: corneal epithelium removed; * Commercial product not available, prepared by pharmacist.

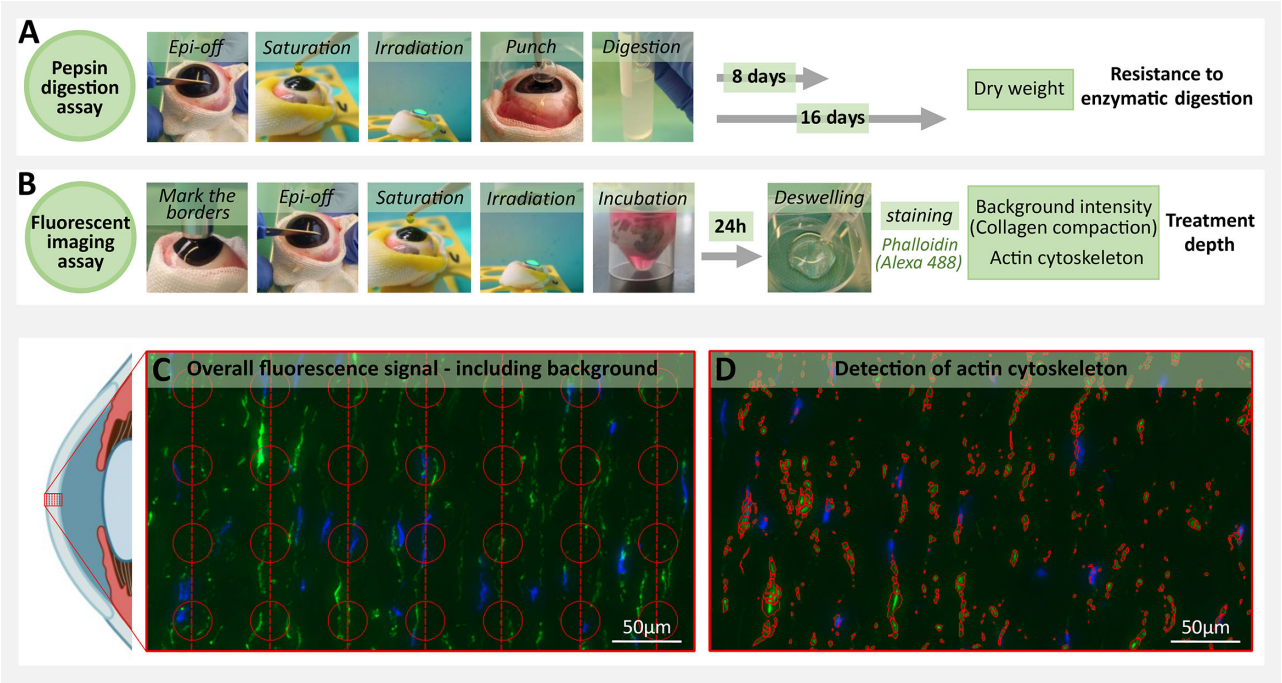

Figure 2. **Pepsin digestion and fluorescent imaging assay protocols.** (**A**) Pepsin digestion assay: main protocol steps during tissue processing and end point assessment via sample dry weight measurements at day 8 or 16. (**B**) Fluorescent imaging assay: main protocol steps during tissue processing and end point assessment via background intensity and cytoskeleton intensity measurement. (**C**) Evenly sized and spaced sampling regions were identified to measure the overall Alexa 488 fluorescence signal (both background and cytoskeletal actin fluorescence) as a measure of stromal collagen compaction. (**D**) Cytoskeletal actin was identified via segmentation in the Alexa 488 channel; The anterior eye segment was adapted from the icon "Sagittal eye (simplified)", by BioRender.com, 2022 (www.app.biorender.com).

ments were performed to quantify corneal resistance to enzymatic digestion, according to previously described methods.[51,52,56,57]

Time to complete digestion and changes in corneal button diameter have been used as end points to quantify corneal resistance to enzymatic digestion in previous publications.[38,51,52] Neither of these end points were used in this study, because tissue fragmentation and turbidity of the pepsin solution increased with incubation time. As a result, tissue presence could not be quantified objectively after 20 days of incubation, significantly biasing the parameters "time to complete digestion" and "changes in corneal button diameter."

Fluorescent Imaging Assay

- **Sample Preparation**

After PACK-CXL treatment, eyes were incubated in cell culture medium (ThermoFisher Scientific, MEM alpha, no nucleosides, catalog no. 22561021) for 24 hours at 20°C, with the cornea raised above the culture medium surface. Following incubation, the corneas were dissected, bisected, and placed in a 20% dextran solution for 45 minutes to reduce tissue swelling. The corneas were subsequently washed and cryopreserved. Six µm thick cryosections of each cornea were placed onto positively charged glass slides and further processed for fluorescent biomarker staining with DAPI (ProLongTM Diamond Antifade Mountant with DAPI; ThermoFisher Scientific) and phalloidin (Alexa Fluor 488 phalloidin; ThermoFisher Scientific), according to product guidelines (full fluorescent biomarker staining protocol available as Supplement C).

- **Fluorescent Imaging and Image Analysis**

Samples were imaged using a slide scanner (Digital Slide Scanner 3D Histech Pannoramic 250). Three cutouts of the treated central cornea were prepared per image using QuPath-0.2.3.[58] All cutouts were oriented with the anterior side of the cornea on the left side of the image in Image J 1.53a (see Figs. 2c, 2d). The boundary between slide surface and deepithelialized cornea was manually marked to define the region of interest used for image analysis. An additional cutout from the untreated, peripheral, epithelialized cornea was prepared from each image as negative control. A dedicated CellProfiler[59] pipeline, available at GitHub repository under https://github.com/sstoma/ia-project-ems, was created to further process images for data analysis. Collagen compaction and changes to the nuclear morphology and actin cytoskeleton of keratocytes in the anterior corneal stroma have previously been described as a result of epithelium-off CXL.[31,60,61] Cytoskeletal actin was identified in the Alexa 488 channels, by segmenting objects using the IdentifyPrimaryObjects module (see Fig. 2d). In addition, evenly sized and spaced sampling regions were identified to measure the overall Alexa 488 fluorescence signal, including both background and cytoskeletal actin fluorescence, as a measure of stromal collagen compaction (see Fig. 2c). The final segmentation and its parameters were confirmed via visual inspection of the output. Images in which automatic segmentation resulted in too many artifacts were excluded from the final analyses (details of the selection available at GitHub repository under https://github.com/sstoma/ia-project-ems). As a result, 52 of 423 images were excluded from the cytoskeletal actin identification dataset. Different morphometric and intensity-based features were computed for objects identified in the channels of interest and correlated to their distance from the anterior tissue edge. We created an additional computational channel, in which Alexa 488 was cleaned using background subtraction implemented in ImageJ.[62]

- **Data Analysis of CellProfiler Output**

Analysis of CellProfiler output was performed with Python using Pandas,[63] and plots were created using the Seaborn[64] library. The script is provided at GitHub repository under https://github.com/sstoma/ia-project-ems. Data analysis was performed on cytoskeletal actin identification, and background and cytoskeletal actin fluorescence measurement data originating from the corneal tissue between 50 and 800 µm from the corneal surface.

Stromal collagen compaction was analyzed based on the intensity of the nonspecific background phalloidin-Alexa 488 fluorescence signal. The mean object counts were also analyzed in the phalloidin-Alexa 488 channel. The cytotoxic post-CXL effect was evaluated based on cytoskeletal fragmentation by counting the number of objects labeled with mean gray value intensities above the Alexa 488 channel threshold.

- **Automatic Computation of the Estimated Treatment Depth**

Assessment of the PACK-CXL treatment depth was based on the estimated collagen compaction depth. Treatment depth was estimated by computing a derivative of smoothed phalloidine background intensity values, aggregated by averaging different images of the same experimental condition, as a function of distance from the tissue edge. Computed derivative values were compared to an empirically established threshold. The first distance measurement from the endothelial side of the tissue sections for which the derivative reached a smaller value than the threshold was assumed to represent the PACK-CXL penetration depth. We assume this algorithm to identify the tissue depth at which structural collagen changes cease to be identified and collagen compaction stops. The details of this procedure are available in the GitHub repository under https://github.com/sstoma/ia-project-ems. To ensure the robustness of this analysis, we checked different thresholds and observed that the choice of threshold (within a reasonable range) does not change

the qualitative results when comparing between conditions.

Temperature Assay

The temperature of the corneal surface was measured eight times with an infrared thermometer in four porcine eyes that underwent an accelerated, high fluence PACK-CXL protocol. See Supplement B for experimental protocol details.

Experimental Layout

Six hundred eighty-eight corneas were used in the pepsin digestion assay, divided in five experiments. These experiments were performed in batches of 20 to 30 eyes, which were processed during the same day. In each batch, the corneas were randomly allocated to the control group or one of the various treatment groups representing the PACK-CXL protocol modifications investigated. In experiment 1 (acceleration), a 10 minute 9 mW, and 2 minute 45 mW protocol were compared to a 30 minute 3 mW, 5.4 J/cm^2 protocol (135 corneas). In experiment 2 (fluence), 10.8, 16.2, 21.6, 26, and 32.4 J/cm^2 protocols were compared to a 10 minute 9 mW, 5.4 J/cm^2 protocol (263 corneas). In experiment 3 (riboflavin concentration and D_2O supplementation), 0.1 and 0.4% riboflavin concentrations were compared, and the supplementation of D_2O was evaluated, using a 10 minute 9 mW, 5.4 J/cm^2 protocol (125 corneas). In experiment 4 (riboflavin carrier), HPMC was compared to Dextran as chromophore carrier using a 10 minute 9 mW, 5.4 J/cm^2 protocol (122 corneas). In experiment 5 (riboflavin replenishment), two 10 minute 9 mW + 2 × 2 minutes 45 mW, 16.2 J/cm^2 protocols were compared, during which riboflavin was either replenished during and between irradiation cycles, or not (41 corneas). See Tables 1a and 1b for the detailed experimental layout.

Information gathered in the pepsin digestion assay allowed us to select promising PACK-CXL parameters for the fluorescent imaging assay. Based on the results, we selected the 10 minute 9 mW, 5.4 J /cm^2 PACK-CXL protocol as the reference protocol. The following treatment groups were evaluated in the fluorescent imaging assay: (control epi-on) epithelium untouched (25 corneas); (control epi-off) epithelium removed (86 corneas); (fluence 5.4 J/cm^2) a 10 minute 9 mW, 5.4 J/cm^2 fluence protocol (33 corneas); (fluence 5.4 J/cm^2 and 0.4% riboflavin) 0.4% riboflavin, a 10 minute 9 mW, 5.4 J/cm^2 fluence protocol (14 corneas); (fluence 5.4 J/cm^2, HPMC) HPMC as a carrier, a 10 minute 9 mW, 5.4 J/cm^2 fluence protocol (12 corneas); (fluence 16.2 J/cm^2) a 10 minute 9 mW + 2 × 2 minutes 45 mW, 16.2 J/cm^2 protocol (14 corneas); (fluence 16.2 J/cm^2, no riboflavin replenishment) a 10 minute 9 mW + 2 × 2 minutes 45 mW, 16.2 J/cm^2 protocol, where riboflavin was not replenished during and between irradiation cycles (12 corneas).

Data Analysis

Linear models were built to assess whether treatment type has an effect on corneal dry weight at day 8 (DW8) or day 16 (DW16). The model was adjusted for two variables: (1) CCT measurements after riboflavin saturation, and (2) date at which corneas were processed. The outcomes–DW8 and DW16–were analyzed separately for each experiment. Differences between specific treatment groups were assessed via Tukey's "Honest Significant Difference" method. The sample sizes needed to detect differences in mean corneal weight between treatment groups were calculated based on reported standard deviations (SD of 7,[57] SD of 1,[52] and SD of 0.24[56]), and a power of 80% and type 1 error of 5% were assumed. The minimum sample group size was six corneas per treatment group.

The statistics program R 3.1.2., with packages multcomp and nlme were used for all statistical calculations. Data sets and R scripts are available at the GitHub (https://github.com/sstoma/ia-project-ems).

Results

General Results

The average CCT of corneas in treatment groups saturated with riboflavin/dextran solution was significantly lower than the CCT of control group corneas that were not exposed to any riboflavin solution ($P < 0.001$, 95% confidence interval [CI] from 107 to 113). The average CCT of corneas saturated with riboflavin/HPMC solution did not significantly differ from the CCT of control group corneas. There was no significant difference between treatment groups in average CCT after saturation with riboflavin/dextran solution. These results are presented in Supplementary Table S1.

- **Pepsin Digestion Assay**

As described in previous reports, the pepsin-incubated tissue samples initially swelled and then separated into an anterior and posterior part.[37,38] This process was followed by the rapid digestion of the posterior part and preservation of the cross-linked anterior part.

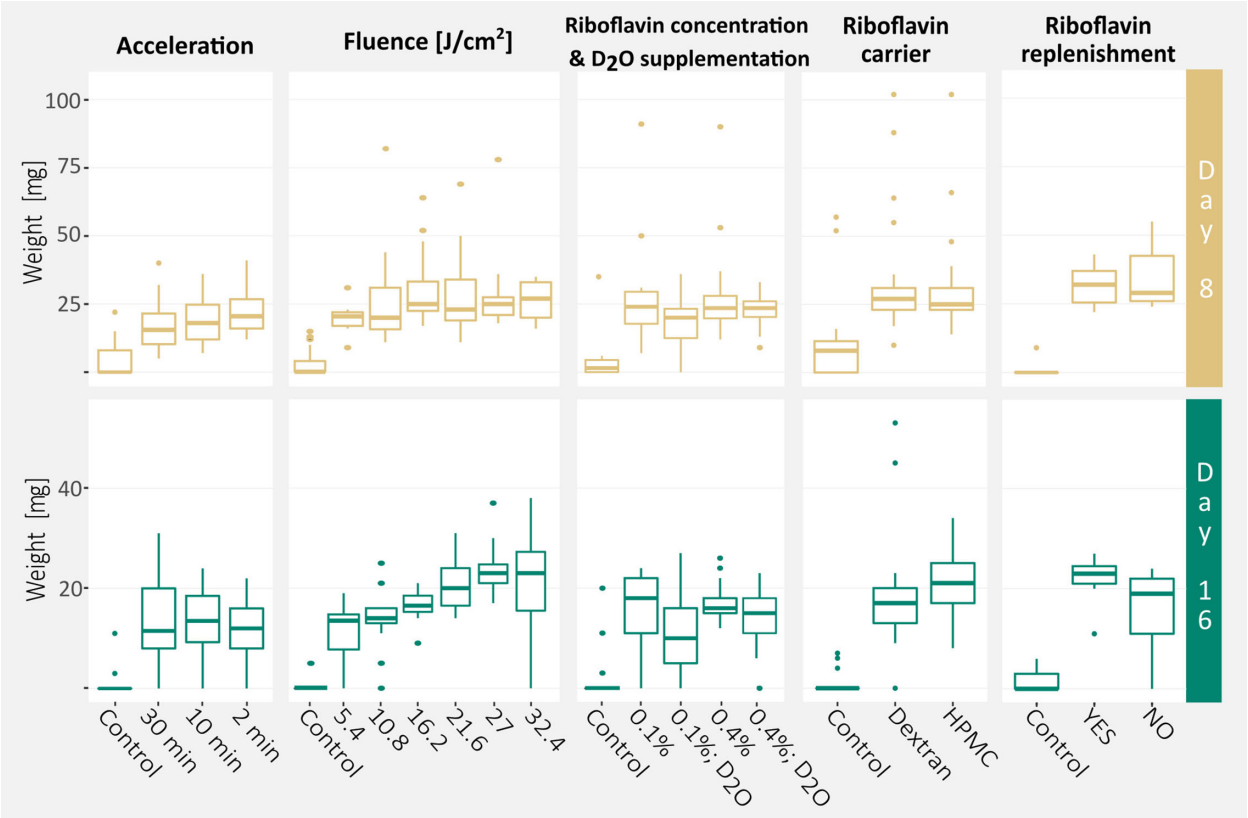

Figure 3. Effects of PACK-CXL protocol modification on corneal resistance to enzymatic digestion. Dry weight measurements at days 8 and 16, as quantification of corneal resistance to enzymatic digestion, and its distribution between experiments and experimental conditions, presented as boxplots. The *bold horizontal line* represents the median, and the *lower and upper horizontal lines* represent the first and third quartile of the data, respectively.

All PACK-CXL treated groups, expect for the 0.1% riboflavin and D_2O supplemented corneas, had a significantly greater DW8 compared to untreated controls. All PACK-CXL treated groups had a significantly greater DW16 compared to untreated controls, regardless of the PACK-CXL protocol parameters (Fig. 3). Greater differences in DW16 than in DW8 were observed between treatment groups (Table 2).

In our analysis, 5 specific days on with corneas were processed, had a significant impact on sample weight, either decreasing or increasing it. We expect that the age and/or housing conditions of animals slaughtered on these specific days, and/or experimental settings, such as ambient temperature and humidity during sample preparation and other indeterminate conditions, might have played a role.

- **Fluorescent Imaging Assay**

We assessed the effects of PACK-CXL by combining information from three graphs: background and cytoskeleton fluorescence intensity, and phalloidin stained object counts (Fig. 4). Background fluorescence provided information regarding stromal collagen compaction intensity and depth. However, because this parameter combines signal intensities from both collagen and the cytoskeleton, a comparison to two other parameters, cytoskeleton fluorescence intensity and cytoskeleton object count, was needed. All PACK-CXL treated corneas demonstrated increased background fluorescence in the anterior corneal stroma (see Fig. 4) when compared to both controls. Within this area of increased collagen compaction, we observed a peak in cytoskeleton fluorescence intensity combined with a decrease in number of phalloidin-stained cytoskeletal objects, suggesting PACK-CXL induced cytotoxicity (cytoskeletal fragmentation and increased fluorescence as a result of apoptotic cell death; see Fig. 4). This was not observed in the control samples. A gradual decrease in background and cytoskeleton fluorescence, and in phalloidin stained objects counts, from anterior to posterior stroma was observed in the Epi-on group. This is

Table 2. Dry Weight Measurements of Samples After 8 or 16 Days of Incubation in Pepsin Solution

Experiments	Sample Dry Weight	
	Day 8 [µg]	Day 16 [µg]
Acceleration		
Control	4.9 ± 7.3 (0–22)	1.2 ± 3 (0–11)
30 min	17.5 ± 97 (5–40)	13.8 ± 8.5 (0–31)
10 min	18.5 ± 7.9 (7–36)	13.1 ± 7.9 (0–24)
2 min	22.3 ± 8.1 (12–41)	11.9 ± 6.8 (0–22)
Fluence		
Control	2.7 ± 4.6 (0–15)	0.2 ± 0.9 (0–5)
5.4 J/cm^2	20.2 ± 5.4 (9–31)	11.7 ± 6 (0–19)
10.8 J/cm^2	26.9 ± 17.8 (11-82)	13.8 ± 6 (0–25)
16.2 J/cm^2	30.2 ± 13.3 (17–64)	16.6 ± 3 (9–21)
21.6 J/cm^2	26.6 ± 12.3 (11–69)	20.6 ± 4.7 (14–31)
27 J/cm^2	28.8 ± 14.7 (18–78)	23.4 ± 5.1 (17–37)
32.4 J/cm^2	26 ± 7 (16–35)	21.4 ± 9.5 (0–38)
Riboflavin concentration and D_2O supplementation		
Control	4.8 ± 9.8 (0–35)	2.6 ± 6.1 (0–20)
0.1 riboflavin	29.1 ± 22.4 (7–91)	15.8 ± 7.2 (0–24)
0.1 riboflavin; D_2O	18.8 ± 10.1 (0–36)	11.5 ± 8.4 (0–27)
0.4 riboflavin	30 ± 21.9 (12–90)	17.2 ± 4.4 (12–26)
0.4 riboflavin; D_2O	22.7 ± 7.1 (9–33)	14 ± 6.3 (0–23)
Riboflavin carrier		
Control	11.2 ± 16.2 (0–57)	0.9 ± 2.2 (0–7)
HPMC	35.1 ± 23.2 (10–102)	18.5 ± 11.5 (0–53)
Dextran	31.2 ± 19.6 (14–102)	20.7 ± 6.2 (8–34)
Riboflavin replenishment		
Control		1.7 ± 2.9 (0–6)
Yes	31.7 ± 7.8 (22–43)	21.7 ± 5.2 (11–27)
No	35 ± 12.1 (24–55)	15.5 ± 9 (0–24)

Data presented as mean ± standard deviation (minimum – maximum).

likely caused by the higher keratocyte density in the normal anterior, compared to the posterior, corneal stroma, as has been observed in human, rabbit, and feline corneas.[65–67] Corneas in the Epi-off group demonstrated the same background fluorescence, and phalloidin stained objects counts, in the anterior and posterior stroma. The cytoskeleton fluorescence in the anterior stroma was stunted, when compared to the corneas in the Epi-on group. It is conceivable that keratocyte apoptosis as a result of epithelial debridement caused the decreased cytoskeleton fluorescence and phalloidin stained object counts, and by extension, the decreased overall background fluorescence, in the anterior stroma of corneas in the epi-off group, compared to corneas in the epi-on group.[68,69]

We observed decreased collagen compaction in samples with a small amount of remaining epithelium, compared to other samples in the same group. We demonstrated an effect depth of approximately 400 µm (anterior 50% of the stroma) following treatment with a 10 minute 9 mW, 5.4 J/cm^2 PACK-CXL protocol (see Fig. 4), which is comparable to previously published data.[31,61,70,71]

PACK-CXL Protocol Modifications

The PACK-CXL treatment effects are summarized in Figure 3 (sample dry weight measurements – stromal resistance to enzymatic digestion) and Figure 4 (fluorescent signal intensity–treatment depth). Estimated average treatment effects and differences between treatment groups for sample dry weight measurements are presented in the Supplementary Tables S2 and S3.

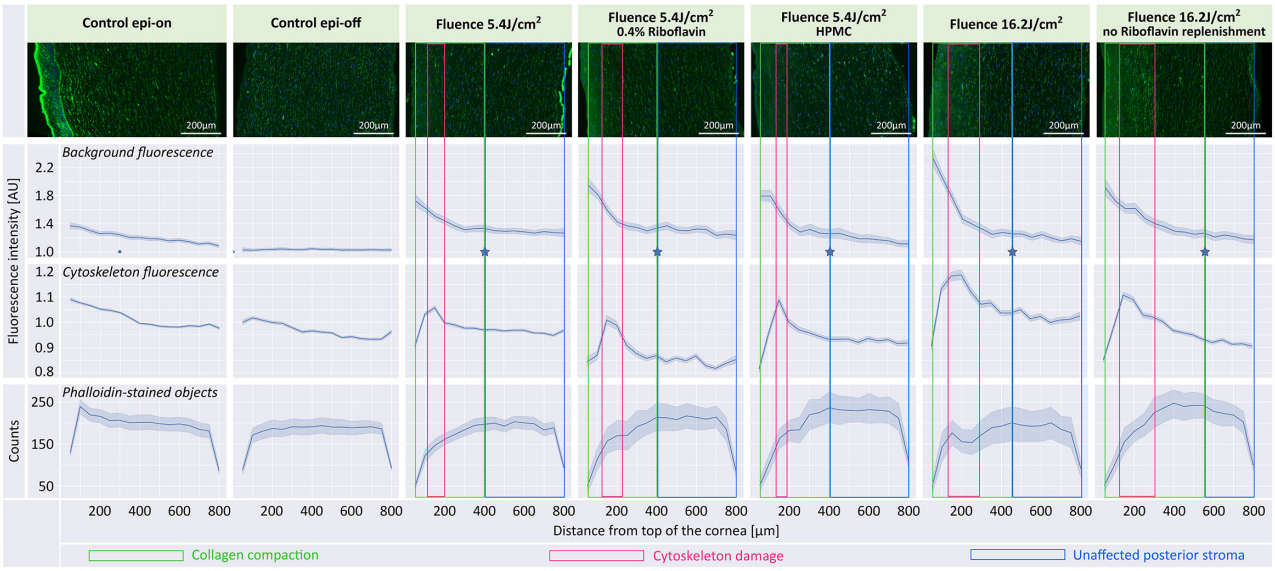

Figure 4. **Effects of PACK-CXL modifications on treatment depth.** *Top row of graphs*: Overall fluorescent signal intensity, including background, as a function of distance from the anterior corneal stromal surface. *Middle row of graphs*: Actin cytoskeleton fluorescent signal intensity, no background, as a function of distance from the anterior corneal stromal surface. *Bottom row of graphs*: Phalloidin stained object (actin cytoskeleton) counts as a function of distance from the anterior corneal stromal surface. The *light blue intervals in the graphs* are 95% confidence intervals computed by grouping images. The *blue stars* in the background fluorescence graphs represent the transition between the anterior zone of collagen compaction (*boxed in green areas*), and the unaffected posterior stroma (boxed in blue areas). Placement of the *blue stars* is based on computed derivative values, and assumed to indicate the PACK-CXL treatment depth. The treatment group "Fluence 16.2 J/cm^2 no Riboflavin replenishment" demonstrates the deepest treatment effect. A decrease in phalloidin-stained object counts and a peak in cytoskeleton fluorescence (*boxed in pink areas*) are visible in the anterior stroma in all PACK-CXL treated groups. These changes are likely related to PACK-CXL treatment-induced cell damage and cell loss. AU, arbitrary units.

- **Acceleration**

Acceleration of the PACK-CXL treatment had no effect on DW8 or DW16. Statistical modeling demonstrated that the CCT after riboflavin saturation had an effect on DW8 and DW16. A CCT increase of 100 µm led to an estimated average increase in DW8 and DW16 of 4 and 6 µg, respectively ($P = 0.02$, 95% CI from 0.5 to 8; and $P = 0.002$, 95% CI from 2 to 10).

- **Fluence**

No differences in DW8 between PACK-CXL treated groups were observed. However, significant differences in DW16 were observed between groups treated with different PACK-CXL fluences. Corneas treated with 21.6 J/cm^2, 27 J/cm^2, and 32.4 J/cm^2 fluence protocols had a significantly greater DW16 compared to 5.4 J/cm^2 and 10.8 J/cm^2 fluence protocol-treated corneas (see Supplementary Table S3). Similarly, 27 J/cm^2 protocol-treated corneas had a significantly greater DW16 than 16.2 J/cm^2 fluence protocol-treated corneas (see Supplementary Table S3). We emphasize that 32.4 J/cm^2 fluence protocol-treated corneas were often fragmented at day 16, which is reflected in the high variation in DW16 (see Table 2). Statistical modeling demonstrated that the CCT after riboflavin saturation had an effect on DW16. A CCT increase of 100 µm led to an estimated average increase in DW16 of 3 µg ($P = 0.007$, 95% CI from 0.8 to 4).

Groups treated with 5.4 J/cm^2 and 16.2 J/cm^2 fluence protocols demonstrated a similar depth of collagen compaction. However, corneas that received a 16.2 J/cm^2 fluence protocol showed an increased intensity of background fluorescence, indicating more intense collagen compaction, and a broader peak of increased cytoskeleton fluorescence, indicating a wider zone of cytoskeletal damage, compared to corneas that received one third of the PACK-CXL fluence (5.4 J/cm^2 protocol).

- **Riboflavin Concentration and D_2O Supplementation**

All PACK-CXL treated groups had a significantly greater DW8 compared to the control group, except for the treatment group that was saturated with 0.1% riboflavin and D_2O. All PACK-CXL treated groups

had a significantly greater DW16 compared to the control group. A dry weight increase compared to the 0.1% riboflavin saturated group was not observed in PACK-CXL treated corneas that received 0.4% riboflavin, D_2O supplementation, or both (see Supplementary Table S3).

The group of corneas that was saturated with 0.4% riboflavin demonstrated a similar depth of collagen compaction with a minimal increase in collagen compaction when compared to a 0.1% riboflavin, 5.4 J/cm^2 group. All 5.4 J/cm^2, 9 mW protocol treated groups showed comparable cytotoxic effects.

- **Riboflavin Carrier**

No difference in DW8 or DW16 was observed between PACK-CXL treated groups saturated with riboflavin/dextran or with riboflavin/HMPC. Statistical modeling demonstrated that the CCT after riboflavin saturation had an effect on DW8. A CCT increase of 100 µm led to an estimated average increase in DW8 of 15 µg ($P = 0.012$, 95% CI from 3.3 to 26). Corneas that were saturated with HPMC instead of dextran demonstrated no increase in depth or intensity of collagen compaction, nor of cytotoxic effects.

- **Riboflavin Replenishment**

No statistically significant difference in DW8 or DW16 was observed between PACK-CXL treated groups that received riboflavin replenishment during and between irradiation cycles, and those that did not. However, the DW16 measurements of the PACK-CXL treated corneas that did not receive riboflavin replenishment ranged from 0 to 24 µg, whereas DW16 for the corneas that received riboflavin replenishment ranged from 11 to 27 µg (see Table 2). In addition, the PACK-CXL treated corneas (16.2 J/cm^2 fluence protocol) that did not receive riboflavin replenishment demonstrated reduced collagen compaction in the anterior corneal stroma but a deeper treatment effect, compared to the corneas that received riboflavin replenishment and 16.2 J/cm^2 fluence PACK-CXL. The no riboflavin replenishment with 16.2 J/cm^2 fluence PACK-CXL protocol demonstrated a deeper treatment effect than any of the other tested protocols.

Temperature Assay

The corneal surface temperature did not change significantly with increasing amounts of PACK-CXL energy delivered. Surface temperature measurements are presented as Supplementary Figure S1.

Discussion

In this study, we explored various PACK-CXL protocol modifications to help select simple, short, and effective PACK-CXL protocols that provide a high corneal resistance to enzymatic digestion (corneal stromal stability) and adequate treatment depth during clinical use.

Contrary to what we had hypothesized, acceleration did not appear to have a deleterious impact on the stability of the corneal stroma. As anticipated, we observed greater corneal stromal stability, and strong collagen compaction but unchanged treatment depth with an increase in fluence. Contrary to our hypotheses, neither the use of 0.4% riboflavin, supplementation with D_2O, nor the choice of riboflavin carrier, had any effect on treatment depth or PACK-CXL-induced corneal stromal stability. Finally, and as anticipated, omission of riboflavin replenishment during and between irradiation cycles resulted in a deeper but less intense treatment effect. The latter finding seems to be confirmed by the higher variability in stromal collagen resistance to enzymatic degradation in this treatment group.

Previous reports, in which the effect of PACK-CXL acceleration on corneal resistance to enzymatic digestion was investigated, demonstrated conflicting results. PACK-CXL acceleration up to 5 minutes at 18 mW/cm^2 did not alter tissue digestion time compared to a 30 minute 3 mW/cm^2 and a 10 minute 9 mW/cm^2 protocols in 2 studies,[38,72] which is in line with our findings. However, tissue digestion time was reduced by PACK-CXL acceleration in other studies.[52,73] Likewise, in our hands, the use of a 0.4% riboflavin solution did not increase stromal resistance against enzymatic degradation, compared to the use of a 0.1% riboflavin solution. We were thus not able to replicate previous findings, where dry weight measurements of 0.3% riboflavin saturated corneas were higher compared to 0.1% riboflavin saturated corneas.[56]

We cannot definitively explain the differences between these reported and our results. It is likely that the following aspects influence the reproducibility of and the discrepancies in the results. First, differences in laboratory conditions, animal population, and equipment and reagents used, may have affected the results. Because we used laboratory equipment that was available to us, we did not completely copy previously reported digestion assays. Second, for reasons given in the Materials and Methods section, we used a different primary outcome measurement and statistical analysis in our digestion assay than was reported by previous groups. This can lead to different conclusions.

For example, weight is a continuous outcome measurement, for which linear models are appropriate, whereas time to complete tissue digestion is suitable for survival analysis. Finally, a statistical phenomenon called replication power should be considered. Here, the probability to obtain significant results in replication studies that confirm the original study is only 50%, if the original study had a *P* value of 0.05.[74] Furthermore, there is no current agreement on digestion assay settings that are appropriate for evaluating the impact of PACK-CXL on stromal resistance against enzymatic degradation.

Our finding that elevation of PACK-CXL fluence increases corneal stromal resistance against enzymatic digestion[52,75] is in agreement with previous reports. However, this trend has its limits. We observed a plateau in tissue dry weight measurements at energy levels of 21.6 J/cm^2 and higher. Similarly, the antibacterial effect of PACK-CXL increases with increasing fluence[40,41,43,76] with a 100% in vitro antibacterial effect at fluences of 16.2 J/cm^2 and higher.[43] These combined results suggest that patients may not benefit from the use of fluences above 21.6 J/cm^2. In fact, tissue fragmentation and a very high variance in dry weight measurements were observed in the group of corneas that received a fluence of 31.4 J/cm^2 in our study. We believe that the structural integrity of the cornea may be irreversibly damaged at such high fluence levels.

A concern has been raised that high energy levels might create heat that could lead to collagen denaturation and damage ocular structures.[77,78] We demonstrated that the corneal surface temperature does not change significantly as more energy is delivered during PACK-CXL.

Our results, together with information available in the literature, suggest that PACK-CXL protocols with a fluence around 16.2 J/cm^2 to 21.6 J/cm^2 could be very useful and are most likely safe to be used as treatment for infectious keratitis.[79,80] Such protocols eradicate the majority of bacteria,[42,43,81] and substantially increase corneal resistance to enzymatic digestion at the same time.

The observed deeper but less intense PACK-CXL treatment effect as a result of not replenishing riboflavin during the irradiation phase, can potentially be explained as follows. As riboflavin is used in the photopolymerization process, riboflavin concentrations in the superficial stroma will decrease, allowing UVA to reach and induce cross-linking in deeper layers of the stroma,[82] increasing treatment depth. At the same time, riboflavin likely diffuses from the deeper stromal layers to the superficial treatment area, resulting in a generalized depletion of riboflavin in the tissue, resulting in a decreased and more variable overall level of tissue crosslinking in the "no riboflavin replenishment" compared to the "riboflavin replenishment" scenario.

There are a few limitations to our study. First, because in vitro and ex vivo results do not necessarily translate to in vivo situations, we cannot predict whether the PACK-CXL protocols that we evaluated ex vivo, will perform similarly in clinical cases. For example, the presence of secondary changes, such as corneal opacification, as a result of inflammatory cell infiltrates or edema, may reduce UVA absorption and PACK-CXL effectivity. In addition, the ex vivo pepsin digestion assay is a simplification of the enzymatic tissue degradation that occurs in vivo. A compelling case can be made that the use of collagenase enzymes, as described in a number of publications,[37,72,73,83,84] is a more realistic representation of the in vivo situation. However, because CXL triggers cross-linking within collagen fibrils, but also between collagen fibrils and other corneal stromal matrix components,[34,35] we chose pepsin as the proteolytic enzyme instead of collagenase. This choice also enables a comparison to relevant previously published data.[38,52]

Moreover, the quantification method that we used in our fluorescent imaging assay has typical limitations due to the nature of fluorescent microscopy,[85] including intrinsic and extrinsic noise, and image variability. To minimize the influence of image variability, we have normalized the fluorescent intensity values per image, instead of directly comparing raw values.

Last, we would like to emphasize that this study has a hypothesis generating nature, which comes with certain shortcomings, especially because certain potentially effective protocol modifications were disqualified when not demonstrating effect increases under the experimental conditions used in this study. In order to determine the most optimal PACK-CXL settings and not miss potentially effective protocol modifications, variables like riboflavin concentration, supplementation with D_2O, and the use of HPMC, should likely be tested across energy levels.

Conclusions

Our study complemented previously published reports on PACK-CXL protocol modification by exploring new possible protocol adjustments, thus generating data that help to determine optimized clinical PACK-CXL settings and direct future research efforts. We conclude that increased PACK-CXL fluence improves corneal resistance to enzymatic digestion. However, protocols that deliver energy levels above 27 J/cm^2 are unlikely to benefit patients and might

increase the risk for negative treatment side-effects. PACK-CXL acceleration is unlikely to have a negative effect on corneal resistance to enzymatic digestion and facilitates the delivery of high fluence protocols, whereas at the same time decreasing the duration of treatment. Finally, riboflavin may not need to be replenished after the initial stromal saturation phase.

Acknowledgments

Supported by an ECVO Research Grant, an ACVO Vision for Animals Foundation (VAF) Founders Clinical Research Grant, and a BrAVO Research Grant. Peschke Trade kindly supported this study by donating the riboflavin solutions. The laboratory work was performed using the logistics of the Center for Clinical Studies at the Vetsuisse Faculty of the University of Zurich.

Funding information: European College of Veterinary Ophthalmologists Research Grant, American College of Veterinary Ophthalmologist Vision for Animals Foundation (VAF) Founders Clinical Research Grant, British Association of Veterinary Ophthalmologists Research/Travel Grant.

Disclosure: **M. Kowalska**, (N); **E. Mischi**, (N); **S. Stoma**, (N); **S.F. Nørrelykke**, (N); **S. Hartnack**, (N); **S.A. Pot**, (N)

* MK and EM are joint first authors.

References

1. Chan C. Corneal cross-linking for keratoconus: Current knowledge and practice and future trends. *Asia Pac J Ophthalmol (Phila)*. 2020;9(6):557–564.
2. Ting DSJ, Henein C, Said DG, Dua HS. Photoactivated chromophore for infectious keratitis – Corneal cross-linking (PACK-CXL): A systematic review and meta-analysis. *Ocul Surf*. 2019;17(4):624–634.
3. Papaioannou L, Miligkos M, Papathanassiou M. Corneal collagen cross-linking for infectious keratitis: A systematic review and meta-analysis. *Cornea*. 2016;35(1):62–71.
4. Pot SA, Gallhöfer NS, Matheis FL, Voelter-Ratson K, Hafezi F, Spiess BM. Corneal collagen cross-linking as treatment for infectious and noninfectious corneal melting in cats and dogs: Results of a prospective, nonrandomized, controlled trial. *Vet Ophthalmol*. 2014;17(4):250–260.
5. Shukla AK, et al. Photoactivated Chromophore for Keratitis–Corneal Cross-linking (PACK-CXL): Retrospective, multicenter study in canine and feline patients. *Vet. Ophthalmol*. 2023;00:1–36.
6. Shetty R, D'Souza S, Khamar P, Ghosh A, Nuijts RMMA, Sethu S. Biochemical markers and alterations in keratoconus. *Asia Pac J Ophthalmol (Phila)*. 2020;9(6):533–540.
7. di Martino E, Ali M, Inglehearn CF. Matrix metalloproteinases in keratoconus – Too much of a good thing? *Exp Eye Res*. 2019;182:137–143.
8. Pahuja N, Kumar NR, Shroff R, et al. Differential molecular expression of extracellular matrix and inflammatory genes at the corneal cone apex drives focal weakening in keratoconus. *Invest Ophthalmol Vis Sci*. 2016;57(13):5372–5382.
9. Ledbetter EC, Gilger BC. Diseases and surgery of the canine cornea and sclera. In: Gelatt KN, Gilger BC, Kern TJ, eds. *Veterinary Ophthalmology*. Ames, Iowa: Wiley-Blackwell; 2013:976–1049.
10. Maggs DJ. Cornea and Sclera. In: Maggs DJ, et al., eds. *Slatter's fundamentals of veterinary ophthalmology*. St. Louis, MO: Elsevier; 2013:184–219.
11. Ollivier FJ. Bacterial corneal diseases in dogs and cats. *Clin Tech Small Anim Pract*. 2003;18(3):193–198.
12. Livingston ET, Mursalin MH, Callegan MC. A pyrrhic victory: The PMN response to ocular bacterial infections. *Microorganisms*. 2019;7(11):537.
13. Narimatsu A, Hattori T, Koike N, et al. Corneal lymphangiogenesis ameliorates corneal inflammation and edema in late stage of bacterial keratitis. *Sci Rep*. 2019;9(1):2984.
14. Yuan X, Mitchell BM, Wilhelmus KR. Expression of matrix metalloproteinases during experimental Candida albicans keratitis. *Invest Ophthalmol Vis Sci*. 2009;50(2):737–742.
15. Kaufman HE. The practical detection of mmp-9 diagnoses ocular surface disease and may help prevent its complications. *Cornea*. 2013;32(2):211–216.
16. Brown D, Chwa M, Escobar M, Kenney MC. Characterization of the major matrix degrading metalloproteinase of human corneal stroma. Evidence for an enzyme/inhibitor complex. *Exp Eye Res*. 1991;52(1):5–16.
17. Spoerl E, Seiler T. Techniques for stiffening the cornea. *J Refract Surg*. 1999;15(6):711–713.
18. Fleiszig SM, Evans DJ. The pathogenesis of bacterial keratitis: Studies with Pseudomonas aeruginosa. *Clin Exp Optom*. 2002;85(5):271–278.
19. Marquart ME, O'Callaghan RJ. Infectious keratitis: Secreted bacterial proteins that mediate corneal damage. *J Ophthalmol*. 2013;2013:369094.

20. Wang AG, Wu CC, Liu JH. Bacterial corneal ulcer: A multivariate study. *Ophthalmologica*. 1998;212(2):126–132.
21. Upadhyay MP, Karmacharya PC, Koirala S, et al. Epidemiologic characteristics, predisposing factors, and etiologic diagnosis of corneal ulceration in Nepal. *Am J Ophthalmol*. 1991;111(1):92–99.
22. Dunlop AA, Wright ED, Howlader SA, et al. Suppurative corneal ulceration in Bangladesh. A study of 142 cases examining the microbiological diagnosis, clinical and epidemiological features of bacterial and fungal keratitis. *Aust N Z J Ophthalmol*. 1994;22(2):105–110.
23. Varaprasathan G, Miller K, Lietman T, et al. Trends in the etiology of infectious corneal ulcers at the F. I. Proctor Foundation. *Cornea*. 2004;23(4):360–364.
24. Tabibian D, Richoz O, Hafezi F. PACK-CXL: Corneal cross-linking for treatment of infectious keratitis. *J Ophthalmic Vis Res*. 2015;10(1): 77–80.
25. Hafezi F, Kanellopoulos J, Wiltfang R, Seiler T. Corneal collagen crosslinking with riboflavin and ultraviolet A to treat induced keratectasia after laser in situ keratomileusis. *J Cataract Refract Surg*. 2007;33(12):2035–2040.
26. Wollensak G, Spoerl E, Seiler T. Riboflavin/ultraviolet-a-induced collagen crosslinking for the treatment of keratoconus. *Am J Ophthalmol*. 2003;135(5):620–627.
27. Wollensak G. Fundamental Principals of Corneal Collagen Cross-Linking. In: Hafezi F, Randleman J, eds. *Corneal Collagen Cross-Linking*. Thorofare, New Jersey, USA: Slack Inc.; 2013:13–17.
28. Wollensak G, Spoerl E, Wilsch M, Seiler T. Keratocyte apoptosis after corneal collagen crosslinking using riboflavin/UVA treatment. *Cornea*. 2004;23(1):43–49.
29. Seiler T, Hafezi F. Corneal cross-linking-induced stromal demarcation line. *Cornea*. 2006;25(9): 1057–1059.
30. Kymionis GD, Grentzelos MA, Plaka AD, et al. Correlation of the corneal collagen cross-linking demarcation line using confocal microscopy and anterior segment optical coherence tomography in keratoconic patients. *Am J Ophthalmol*. 2014;157(1):110–115.e1.
31. Gallhoefer NS, Spiess BM, Guscetti F, et al. Penetration depth of corneal cross-linking with riboflavin and UV-A (CXL) in horses and rabbits. *Vet Ophthalmol*. 2016;19(4):275–284.
32. Mazzotta C, Traversi C, Caragiuli S, Rechichi M. Pulsed vs continuous light accelerated corneal collagen crosslinking: In vivo qualitative investigation by confocal microscopy and corneal OCT. *Eye (Lond)*. 2014;28(10):1179–1183.
33. Bottós KM, Hofling-Lima AL, Barbosa MC, et al. Effect of collagen cross-linking in stromal fibril organization in edematous human corneas. *Cornea*. 2010;29(7):789–793.
34. Hayes S, Kamma-Lorger CS, Boote C, et al. The effect of riboflavin/UVA collagen cross-linking therapy on the structure and hydrodynamic behaviour of the ungulate and rabbit corneal stroma. *PLoS One*. 2013;8(1):e52860.
35. Zhang Y, Conrad AH, Conrad GW. Effects of ultraviolet-A and riboflavin on the interaction of collagen and proteoglycans during corneal cross-linking. *J Biol Chem*. 2011;286(15):13011–13022.
36. Spoerl E, Huhle M, Seiler T. Induction of cross-links in corneal tissue. *Exp Eye Res*. 1998;66(1):97–103.
37. Spoerl E, Wollensak G, Seiler T. Increased resistance of crosslinked cornea against enzymatic digestion. *Curr Eye Res*. 2004;29(1):35–40.
38. Aldahlawi NH, Hayes S, O'Brart DPS, Meek KM. Standard versus accelerated riboflavin-ultraviolet corneal collagen crosslinking: Resistance against enzymatic digestion. *J Cataract Refract Surg*. 2015;41(9):1989–1996.
39. Wollensak G, Spoerl E, Seiler T. Stress-strain measurements of human and porcine corneas after riboflavin-ultraviolet-A-induced cross-linking. *J Cataract Refract Surg*. 2003;29(9):1780–1785.
40. Makdoumi K, Bäckman A, Mortensen J, Crafoord S. Evaluation of antibacterial efficacy of photoactivated riboflavin using ultraviolet light (UVA). *Graefes Arch Clin Exp Ophthalmol*. 2010;248(2): 207–212.
41. Makdoumi K, Bäckman A. Photodynamic UVA-riboflavin bacterial elimination in antibiotic-resistant bacteria. *Clin Exp Ophthalmol*. 2016; 44(7):582–586.
42. Bäckman A, Makdoumi, Mortensen J, Crafoord S. The efficiency of cross-linking methods in eradication of bacteria is influenced by the riboflavin concentration and the irradiation time of ultraviolet light. *Acta Ophthalmol*. 2014;92(7):656–661.
43. Kling S, Hufschmid FS, Torres-Netto EA, et al. High fluence increases the antibacterial efficacy of PACK Cross-Linking. *Cornea*. 2020;39(8):1020–1026.
44. Hafezi F, Hosny M, Shetty R, et al. PACK-CXL vs. antimicrobial therapy for bacterial, fungal, and mixed infectious keratitis: A prospective randomized phase 3 trial. *Eye Vis (Lond)*. 2022;9 (1):2.

45. Ting DSJ, Henein C, Said DG, Dua HS. Effectiveness of adjuvant photoactivated chromophore corneal collagen cross-linking versus standard antimicrobial treatment for infectious keratitis: A systematic review protocol. *JBI Evid Synth*. 2020;18(1):194–199.
46. Zloto O, Barequet IS, Weissman A, Nimni OE, Berger Y, Avni-Zauberman N. Does PACK-CXL change the prognosis of resistant infectious keratitis? *J Refract Surg*. 2018;34(8):559–563.
47. Knyazer B, Krakauer Y, Baumfeld Y, Lifshitz T, Kling S, Hafezi F. Accelerated corneal cross-linking with photoactivated chromophore for moderate therapy-resistant infectious keratitis. *Cornea*. 2018;37(4):528–531.
48. Knyazer B, Krakauer Y, Tailakh MA, et al. Accelerated corneal cross-linking as an adjunct therapy in the management of presumed bacterial keratitis: A cohort study. *J Refract Surg*. 2020;36(4):258–264.
49. Khripun KV, Kobinets YV, Danilov PA, Rozhdestvenskaya ES, Nizametdinova YS. Corneal collagen cross-linking in mixed etiology keratitis treatment: A case of successful use. *Ophthalmol J*. 2021;13(3):87–96.
50. Nateghi Pettersson M, Lagali N, Mortensen J, Jofré V, Fagerholm P. High fluence PACK-CXL as adjuvant treatment for advanced Acanthamoeba keratitis. *Am J Ophthalmol Case Rep*. 2019;15:100499.
51. Aldahlawi NH, Hayes S, O'Brart DPS, O'Brart ND, Meek KM. An investigation into corneal enzymatic resistance following epithelium-off and epithelium-on corneal cross-linking protocols. *Exp Eye Res*. 2016;153:141–151.
52. Aldahlawi NH, Hayes S, O'Brart DPS, Akhbanbetova A, Littlechild SL, Meek KM. Enzymatic resistance of corneas crosslinked using riboflavin in conjunction with low energy, high energy, and pulsed UVA irradiation modes. *Invest Ophthalmol Vis Sci*. 2016;57(4):1547–1552.
53. Hatami-Marbini H, Jayaram SM. Relationship between initial corneal hydration and stiffening effects of corneal crosslinking treatment. *J Cataract Refract Surg*. 2018;44(6):756–764.
54. Hatami-Marbini H, Rahimi A. Stiffening effects of riboflavin/UVA corneal collagen cross-linking is hydration dependent. *J Biomech*. 2015;48(6):1052–1057.
55. Hatami-Marbini H, Jayaram SM. Effect of UVA/riboflavin collagen crosslinking on biomechanics of artificially swollen corneas. *Invest Ophthalmol Vis Sci*. 2018;59(2):764–770.
56. O'Brart NAL, O'Brart DPS, Aldahlawi NH, Hayes S, Meek KM. An investigation of the effects of riboflavin concentration on the efficacy of corneal cross-linking using an enzymatic resistance model in porcine corneas. *Invest Ophthalmol Vis Sci*. 2018;59(2):1058–1065.
57. Aldahlawi NH, Hayes S, O'Brart DPS, Meek KM. Standard versus accelerated riboflavin–ultraviolet corneal collagen crosslinking: Resistance against enzymatic digestion. *J Cataract Refract Surg*. 2015;41(9):1989–1996.
58. Bankhead P, Loughrey MB, Fernández JA, et al. QuPath: Open source software for digital pathology image analysis. *Sci Rep*. 2017;7(1):16878.
59. Stirling DR, Swain-Bowden MJ, Lucas AM, Carpenter AE, Cimini BA, Goodman A. CellProfiler 4: Improvements in speed, utility and usability. *BMC Bioinformatics*. 2021;22(1):433.
60. Bottos KM, Dreyfuss JL, Regatieri CVS, et al. Immunofluorescence confocal microscopy of porcine corneas following collagen cross-linking treatment with riboflavin and ultraviolet A. *J Refract Surg*. 2008;24(7):S715–S719.
61. Esquenazi S, He J, Li N, Bazan HEP. Immunofluorescence of rabbit corneas after collagen cross-linking treatment with riboflavin and ultraviolet A. *Cornea*. 2010;29(4):412–417.
62. Schneider CA, Rasband WS, Eliceiri KW. NIH Image to ImageJ: 25 years of image analysis. *Nature Methods*. 2012;9(7):671–675.
63. Reback J, McKinney W, Van den Bossche J, et al. pandas-dev/pandas: Pandas 1.0.3. 2020, Zenodo. 2020. Available at: https://zenodo.org/record/3715232#.ZFFuzJDMJ_0.
64. Waskom ML. seaborn: Statistical data visualization. *Journal of Open Source Software*. 2021. Available at: https://seaborn.pydata.org/#:~:text=Seaborn%20is%20a%20Python%20data%20visualization%20library%20based,interface%20for%20drawing%20attractive%20and%20informative%20statistical%20graphics. n: statistical data visualization — seaborn 0.12.2 documentation (pydata.org).
65. Patel S, McLaren J, Hodge D, Bourne W. Normal human keratocyte density and corneal thickness measurement by using confocal microscopy in vivo. *Invest Ophthalmol Vis Sci*. 2001;42(2):333–339.
66. Petroll WM, Boettcher K, Barry P, Cavanagh HD, Jester JV. Quantitative assessment of anteroposterior keratocyte density in the normal rabbit cornea. *Cornea*. 1995;14(1):3–9.
67. Twa MD, Giese MJ. Assessment of corneal thickness and keratocyte density in a rabbit model

of laser in situ keratomileusis using scanning laser confocal microscopy. *Am J Ophthalmol*. 2011;152(6):941–953.e1.
68. Wilson SE, Mohan RR, Hong J, et al. Apoptosis in the cornea in response to epithelial injury: Significance to wound healing and dry eye. *Adv Exp Med Biol*. 2002;506(Pt B):821–826.
69. Zieske JD, Guimarães SR, Hutcheon AE. Kinetics of keratocyte proliferation in response to epithelial debridement. *Exp Eye Res*. 2001;72(1):33–39.
70. Li J, Singh M, Han Z, Vantipalli S. A comparison study of Riboflavin/UV-A and Rose-Bengal/Green light cross-linking of the rabbit corneas using optical coherence elastography. In: Proc. SPIE; 2016. Available at: https://www.researchgate.net/publication/299763415_A_comparison_study_of_RiboflavinUV-A_and_Rose-BengalGreen_light_cross-linking_of_the_rabbit_corneas_using_optical_coherence_elastography.
71. Gupta P, Anyama B, Edward K, et al. Depth resolved differences after corneal crosslinking with and without epithelial debridement using multimodal imaging. *Transl Vis Sci Technol*. 2014;3(4):5.
72. Kanellopoulos AJ, Loukas YL, Asimellis G. Cross-linking biomechanical effect in human corneas by same energy, different UV-A fluence: An enzymatic digestion comparative evaluation. *Cornea*. 2016;35(4):557–561.
73. Arafat SN, Robert M-C, Shukla AN, Dohlman CH, Chodosh J, Ciolino JB. UV cross-linking of donor corneas confers resistance to keratolysis. *Cornea*. 2014;33(9):955–959.
74. Held L, Pawel S, Schwab S. Replication power and regression to the mean. *Significance*. 2020;17(6):10–11.
75. Zhu Y, Reinach PS, Zhu H, et al. High-intensity corneal collagen crosslinking with riboflavin and UVA in rat cornea. *PLoS One*. 2017;12(6):e0179580.
76. Shen J, Liang Q, Su G, et al. Effect of ultraviolet light irradiation combined with riboflavin on different bacterial pathogens from ocular surface infection. *J Biophys*. 2017;2017:3057329.
77. Zhu H, Alt C, Webb RH, Melki S, Kochevar IE. Corneal crosslinking with Rose Bengal and green light: Efficacy and safety evaluation. *Cornea*. 2016;35(9):1234–1241.
78. Mencucci R, Mazzotta C, Corvi A, Terracciano L, Rechichi M, Matteoli S. In vivo thermographic analysis of the corneal surface in keratoconic patients undergoing riboflavin–UV-A accelerated cross-linking. *Cornea*. 2015;34(3):323–327.
79. Nordstrom M, Schiller M, Fredriksson A, Behndig A. Refractive improvements and safety with topography-guided corneal crosslinking for keratoconus: 1-year results. *Br J Ophthalmol*. 2017;101(7):920–925.
80. Nicklin A, et al. Safety of high-dose, transepithelial, accelerated CXL with supplemental oxygen on human and monkey eyes. International CXL Experts' Meeting. Zurich; 2018;79. Available at: https://cxlexpertsmeeting.com/wp-content/uploads/2020/03/Program_book_CEM2018_optimized.pdf.
81. Gilardoni F. In-vitro efficacy of accelerated high-fluence PACK-CXL with riboflavin for bacterial keratitis. International CXL Experts' Meeting. Zurich; 2019;65. Available at: https://cxlexpertsmeeting.com/wp-content/uploads/2019/11/Abstract-book-CEM-2019-FINAL-WEB.pdf.
82. O'Brart DPS, O'Brart NAL, Aldahlawi NH, Hayes S, Meek KM. Author Response: The role of riboflavin concentration and oxygen in the efficacy and depth of corneal crosslinking. *Invest Ophthalmol Vis Sci*. 2018;59(11):4451–4452.
83. Kohlhaas M, Spoerl E, Schilde T, Unger G, Wittig C, Pillunat LE. Biomechanical evidence of the distribution of cross-links in corneas treated with riboflavin and ultraviolet A light. *J Cataract Refract Surg*. 2006;32(2):279–283.
84. Fadlallah A, Zhu H, Arafat S, Kochevar I, Melki S, Ciolino JB. Corneal resistance to keratolysis after collagen crosslinking with Rose Bengal and green light. *Invest Ophthalmol Vis Sci*. 2016;57(15):6610–6614.
85. Waters JC. Accuracy and precision in quantitative fluorescence microscopy. *J Cell Biol*. 2009;185(7):1135–1148.
86. Lin JT. The role of riboflavin concentration and oxygen in the efficacy and depth of corneal crosslinking. *Invest Ophthalmol Vis Sci*. 2018;59(11):4449–4450.
87. Lin JT. Influencing factors relating the demarcation line depth and efficacy of corneal crosslinking. *Invest Ophthalmol Vis Sci*. 2018;59(12):5125–5126.
88. Schumacher S, Mrochen M, Spoerl E. Absorption of UV-light by riboflavin solutions with different concentration. *J Refract Surg*. 2012;28(2):91–92.
89. McCall AS, Kraft S, Edelhauser HF, et al. Mechanisms of corneal tissue cross-linking in response to treatment with topical riboflavin and long-wavelength ultraviolet radiation (UVA). *Invest Ophthalmol Vis Sci*. 2010;51(1):129–138.
90. Ehmke T, Seiler TG, Fischinger I, Ripken T, Heisterkamp A, Frueh BE. Comparison of corneal riboflavin gradients using dextran and HPMC solutions. *J Refract Surg*. 2016;32(12):798–802.